



Formulating PEO-polycarbonate blends as solid polymer electrolytes by solvent-free extrusion

Francesco Gambino^{a,b}, Matteo Gastaldi^{a,b}, Alia Jouhara^c, Samuel Malburet^d, Simone Galliano^e, Nicola Cavallini^f, Giovanna Colucci^f, Marco Zanetti^{g,h}, Alberto Finaⁱ, Giuseppe Antonio Elia^{a,b,*}, Claudio Gerbaldi^{a,b,**}

^a GAME Lab, Department of Applied Science and Technology (DISAT), Politecnico di Torino, Corso Duca degli Abruzzi 24, Torino, 10129, Italy

^b National Reference Center for Electrochemical Energy Storage (GISEL) - INSTM, Via G. Giusti 9, Firenze, 50121, Italy

^c BlueSolutions, Odet, Ergué Gabéric, CEDEX 9, 29556, Quimper, France

^d SPECIFIC POLYMERS, 150 Avenue des Cocardières, 34160, Castries, France

^e Department of Chemistry, NIS Interdepartmental and INSTM Reference Centre, University of Torino, Via P. Giuria 7, 10135, Torino, Italy

^f Department of Applied Science and Technology (DISAT), Politecnico di Torino, Corso Duca degli Abruzzi 24, Torino, 10129, Italy

^g Department of Chemistry, SusPlas@Unito – Sustainable Plastic Scientific Hub, University of Turin, via Pietro Giuria 7, 10125, Torino, Italy

^h Instrm Reference Centre, University of Turin, Via G. Quarello 15A, Turin, 10135, Italy

ⁱ Department of Applied Science and Technology (DISAT), Politecnico di Torino, V.le Teresa Michel, 5, 15121, Alessandria, Italy

ARTICLE INFO

Keywords:

Polyethylene oxide
Polycarbonate
Polymer electrolyte
Solid-state battery
Lithium battery
Extrusion

ABSTRACT

Liquid electrolytes are currently state-of-the-art for commercial Li-ion batteries. However, their use implicates inherent challenges, including safety concerns associated with flammability, limited thermal stability, and susceptibility to dendrite formation on the lithium metal anode, that can compromise the battery lifespan. Solid-state polymer electrolytes offer an alternative to conventional liquid electrolytes, aiming to mitigate safety, stability, and performance drawbacks. This study investigates the preparation and the comprehensive characterization of polyethylene oxide (PEO) and polycarbonate (PC) blends obtained through extrusion process. The process is solvent-free and easily scalable at the industrial level; it grants the efficient dispersion and mixing of PEO and PC. Blends at different ratios of PEO (M_w of 4×10^5 and 4×10^6 g mol⁻¹) and two types of PCs (namely, polyethylene and polypropylene carbonate) including lithium bis(trifluoromethanesulfonyl)imide (LiTFSI) are prepared. Optimization and investigation of the relative effects between the application of different PCs and the variable ratios of PEO/PCs on the mechanical, morphologic and electrochemical properties of the final polymeric membranes is carried out for future applications of these systems, as efficient electrolytes in all-solid-state lithium batteries.

1. Introduction

The increasing demand for high-performance, safe, and sustainable energy storage solutions has fueled extensive research into advanced lithium battery technologies, the state-of-the-art power source for mobile electronic applications and electromobility [1–3]. Albeit conventional liquid electrolytes can guarantee the realization of well-performing Li-ion batteries (LIB) [4–8], they contain highly flammable solvents, such as ethers or carbonates, posing significant safety

concerns and limiting their application to an extent [9]. Indeed, the use of liquid electrolytes is not compatible with the fabrication of high energy density batteries with Li-metal anode [10]. Replacing traditional liquid electrolytes with solid-state electrolytes (SSEs) has been regarded as a way to mitigate safety concerns and enable high-energy-density [11–13]. In particular, salt-in-polymer solid polymer electrolytes (SPEs), which are made of a polymeric matrix with dissolved lithium salts, have emerged as promising candidates due to their intrinsic advantages, including improved safety, ease of synthesis, low cost,

* Corresponding author. GAME Lab, Department of Applied Science and Technology (DISAT), Politecnico di Torino, Corso Duca degli Abruzzi 24, Torino, 10129, Italy.

** Corresponding author. GAME Lab, Department of Applied Science and Technology (DISAT), Politecnico di Torino, Corso Duca degli Abruzzi 24, Torino, 10129, Italy.

E-mail addresses: giuseppe.elia@polito.it (G.A. Elia), claudio.gerbaldi@polito.it (C. Gerbaldi).

<https://doi.org/10.1016/j.powera.2024.100160>

Received 15 July 2024; Received in revised form 20 September 2024; Accepted 3 October 2024

Available online 19 October 2024

2666-2485/© 2024 The Authors. Published by Elsevier Ltd. This is an open access article under the CC BY-NC-ND license (<http://creativecommons.org/licenses/by-nc-nd/4.0/>).

flexibility, good electrochemical stability, and compatibility with the roll to roll LIB manufacturing process [14,15]. Thus, polymers, such as polyethylene oxide (PEO), have gained significant attention as polymer matrix since the 1970s. This is ascribed to the oxygen in the polymeric chain being able to coordinate Li^+ , granting a good solubility of lithium salts and the cation hopping mechanism that can move through the polymeric matrix, allowing for good ionic conductivity [16,17]. Despite offering ionic conductivity and compatibility with lithium ions, PEO-based SPEs suffer from limited mechanical strength and electrochemical stability, hindering their widespread adoption in practical applications [18]. In addition, PEO-based electrolytes display a high degree of crystallinity, causing low ionic conductivities for application at temperatures below their melting temperature ($T < 60\text{ }^\circ\text{C}$) [19,20]. Reducing PEO crystallinity is a key strategy to overcome these limitations and advance the development of robust SPEs for lithium batteries [21]. Various strategies have been explored to enhance SPEs for improved ionic conductivity or higher lithium transport number [22]. These include physical methods such as the addition of plasticizers [23], inorganic fillers [24], the blending of different polymers [25] as well as chemical modification like copolymerization [26], crosslinking [27] and the introduction of single-ion polymers [28,29].

As reported in the literature, different families of polymers have been explored as alternatives to PEO for use as SPE matrices. Among these, aliphatic polycarbonates (PCs) are gaining popularity due to their amorphous nature and the similar structure to organic-based solvents employed in traditional electrolytes [30]. PC-based SPEs possess high lithium transference numbers, wide electrochemical stability windows, and compatibility with the lithium metal anode [31]. Some examples of PC-based SPEs, such as poly(trimethylene carbonate) - PTMC [32], poly(ethylene carbonate) - PEC [33] and poly(propylene carbonate) - PPC [34], are already reported in the literature with applications in solid-state batteries. However, polycarbonates exhibit lower ionic conductivity compared to PEO-based electrolytes at low salt concentrations due to the high glass transition temperature (T_g) of the polymer [35]. Sun et al. reported a PTMC-based electrolyte with high electrochemical stability (up to 5.0 V vs. Li/Li^+) but conductivity on the order of 10^{-7} at $60\text{ }^\circ\text{C}$ [36]. Some efforts to combine the properties of PEO with the advantages of PCs are known. Recently, Zhu et al. reported the blending of PEO with PPC. In this case, the polymer showed a decrease in crystallinity, leading to an ionic conductivity in the range of 10^{-4} at $60\text{ }^\circ\text{C}$ [37]. In another example, poly(ethylene ether carbonate) was synthesized through the ring opening of ethylene carbonate. The polymer was completely amorphous, enhancing conductivity to 10^{-4} S cm^{-1} at $40\text{ }^\circ\text{C}$, and the carbonate units improved the stability up to 4.9 V [38].

Our work explores an efficient, scalable, and solvent-free approach to blending PEO with polycarbonates (PC). The study aims to leverage the characteristics of PEO and PC to produce polymeric blends exhibiting an optimal trade-off among ionic conductivity, mechanical strength, and thermal stability, making them suitable for further use as solid polymer electrolytes. The integration of PEO with PCs in a polymer blend seeks to capitalize on the strengths of both polymers, addressing the challenges inherent to PEO-based SPEs. Moreover, the electrolyte blends were prepared using a solvent-free extrusion process. The typical method to prepare polymeric membranes is based on the solvent-based preparation procedure that makes use of organic solvents that, in most cases, are flammable or toxic, such as N-methyl pyrrolidone or dimethylacetamide [39]. Herein, we employed a truly-dry thermal-extrusion process, eliminating the risks associated with flammable solvents, sometimes used for polymer electrolyte preparation, making it an ideal method for the sustainable, fast, and safe development of Li-ion battery SPEs [40]. Extrusion simplifies the manufacturing process, reducing production costs and environmental impact compared to solvent-based methods while obtaining homogeneous and uniform samples, even in case of inclusion of ceramic or inorganic fillers [41,42]. Our research aims to comprehensively investigate the manufacturing, characterization, and performance evaluation of PEO/PC blends for further possible

uses as electrolytes in solid-state Li-based batteries. Materials exhibit an optimal combination of ionic conductivity and electrochemical stability, which is essential for improved safety and performance.

2. Experimental

2.1. Materials

Polyethylene oxide powders (M_w of $4 \cdot 10^5$ and $4 \cdot 10^6\text{ g mol}^{-1}$, respectively, CAS: 25322-68-3) were purchased from Sigma Aldrich. Polyethylene carbonate (PEC, CAS: 25608-11-1) and polypropylene carbonate (PPC, CAS: 25511-85-7) were received from Specific Polymers. Bis(trifluoromethane) sulfonamide lithium salt (LiTFSI) was purchased from Sigma-Aldrich (CAS: 90076-65-6). All polymers were dried for 3 days under vacuum at $60\text{ }^\circ\text{C}$. LiTFSI was dried under vacuum for one day at room temperature, two days at $70\text{ }^\circ\text{C}$, and finally 2 h at $110\text{ }^\circ\text{C}$. Anhydrous N-methyl pyrrolidone (NMP, CAS: 872-50-4) was obtained from Merck and used as received. Conductive carbon C65 (Imerys) and polyvinylidene fluoride (PVDF, Solef 6020, Solvay) were used as received.

2.2. Preparation of PEO/PC blends

A mini-compounder (Haake MiniLab II – Thermo Fischer Scientific) was used to prepare the SPE formulations. The extruder is designed to produce small quantities (approximately 7 cm^3) of polymeric, composite, or nanocomposite materials. The tool consists of two anti-rotational twin screws with controllable rotation speed. The compounder allowed the proper mixing of the polymeric components without using solvents, melting the polymer into the compounder's chamber and recirculating it many times. PEO, PCs, and LiTFSI were weighed in the controlled atmosphere of an Ar-filled MBraun UniLab glove box (H_2O and $\text{O}_2 < 0.5$ ppm). All components were loaded in the mini-extruder with a continuous flow of N_2 to avoid moisture contamination, as the extrusion process was carried out outside the glovebox. Firstly, half of the PEO/PC was introduced in the extruder, then LiTFSI was added little by little, and then the last part of the polymer blend was added. The mixtures were left for 15 min of mixing into the compounder chamber to reach a good homogeneity. The operating conditions during the extrusion were $140\text{ }^\circ\text{C}$ and 130 rpm. After mixing, the blended polymer was extracted from the extruder, sealed under vacuum, and transferred into the glovebox. The final SPEs were obtained by hot-pressing the blended polymer at $70\text{ }^\circ\text{C}$ and 10 bar. Before use, the membranes were dried under vacuum at $40\text{ }^\circ\text{C}$ for 12 h in the B-585 oven (Buchi Glass Drying Oven, Switzerland) and then transferred under vacuum inside the dry glovebox to minimize the presence of residual moisture/humidity. The extrusion process and an example of the resulting membrane are shown in Fig. 1.

2.3. Characterization

The following tests were carried out to characterize the physical, morphological, and electrochemical properties of the polymeric membranes. The thermal stability was measured by thermogravimetric analysis (TGA, Netzsch TG 209 F3), which was conducted between 25 and $600\text{ }^\circ\text{C}$ under a nitrogen atmosphere, using a heating ramp of $10\text{ }^\circ\text{C min}^{-1}$. The temperature at which the degradation process starts was fixed when 5 % ($T_{d5\%}$) of loss in weight was reached. Differential scanning calorimetry (DSC, Netzsch 214 Polyma Equipment) was carried out to evaluate the degree of crystallinity. The measurements were conducted in a temperature range between -50 and $100\text{ }^\circ\text{C}$ with a heating rate of $10\text{ }^\circ\text{C min}^{-1}$ under nitrogen atmosphere (40 mL min^{-1}). The crystallinity degree was calculated as described in Equation (1), using the value of 205 J g^{-1} as melting enthalpy (ΔH_m^0) for 100 % crystalline PEO [43,44].

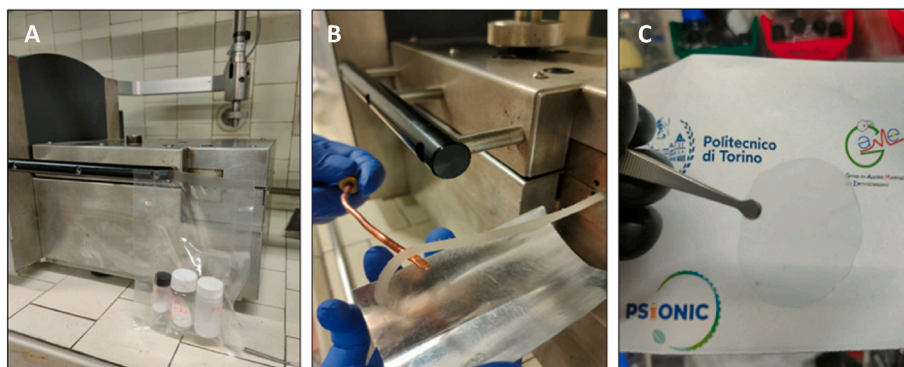


Fig. 1. Different steps of the extrusion process. The precursor materials (A) are introduced into the extruder. After 15 min of mixing at 140 °C and 130 rpm, the blend is extracted from the extruder (B). The formulation is then hot-pressed to obtain the final ready-to-use self-standing SPE (C).

$$\text{Crystallinity (\%)} = \frac{\Delta H_m}{\Delta H_m^0} \times 100 \quad (\text{Eq. 1})$$

The dynamo-mechanical and viscoelastic properties and the relaxation temperatures of the polymer blends were evaluated by dynamic mechanical thermal analysis (DMTA, Q800 by TA Instruments). All measures were carried out applying an isofrequency of 1 Hz with a ramp of temperature from -60 to 60 °C at 3 °C min^{-1} using bar specimens obtained from the above described membranes. From DMTA, storage modulus, loss modulus, and relaxation temperatures (taken as peaks temperature in the loss modulus curves) were obtained. Scanning electron microscopy (SEM, Solaris X, Tescan) was used to characterize the surface and cross-section morphology of the prepared membrane, using a beam energy of 5 keV. Cross-sectional images were obtained by breaking the membranes after having soaked them in liquid nitrogen for 1 min.

The ionic conductivity of the PEO/PC samples was determined by electrochemical impedance spectroscopy (EIS), using a VMP3 potentiostat/galvanostat (Biologic). A membrane disk of 16 mm in diameter, with a thickness of about 150 μm , was sandwiched between two stainless-steel (SS) blocking electrodes in an SS||electrolyte||SS configuration using EL-Cell Std model electrochemical test cells (EL-CELL, Germany). For each SPE, the thickness was accurately measured before and after tests using a micrometer (Mitutoyo). The EIS data were recorded on the VMP-3 electrochemical workstation in a frequency range of 0.1 Hz–1 MHz and applying a sinusoidal voltage of 20 mV at various temperatures (0–80 °C) using an environmentally controlled climatic chamber (MK 53 E2 from BINDER, Germany). The cells were kept for 100 min at each temperature with intervals of 10 °C for proper equilibration. The Nyquist plots were analyzed using Ec-Lab software. The ionic conductivity was determined according to Equation (2):

$$\sigma_i = \frac{D}{AR} \quad (\text{Eq. 2})$$

where D represents the thickness of the membrane (cm), A denotes the area of the membrane (cm^2), and R (Ω) is the total resistance. The electrochemical stability window (ESW) of the PEO/PC blends was measured from the electrochemical linear sweep voltammetry (LSV), considering $5 \mu\text{A cm}^{-2}$ as the threshold and reporting the corresponding E value. The cells were assembled by sandwiching the components in a Li||electrolyte||carbon-coated Al (CC-Al) configuration with a lithium metal (Albemarle) counter and CC-Al working electrode disks. Carbon-coated electrodes were prepared from a slurry containing NMP, conductive carbon C65 (80 % wt.), and PVdF (20 % wt.). The slurry was deposited onto an Al foil, dried overnight at ambient temperature, cut into disks, and vacuum dried at 120 °C for 1 day before use to remove water and residual NMP solvent. The measures were conducted at a scan rate of 1 mV s^{-1} in the range from OCV to 7 V, at the temperature of 40 °C.

2.4. Design of Experiment

The production of polymeric blends involves interplay among various parameters. In this case, we selected three experimental variables (*viz.*, polycarbonate type, polyethylene oxide molecular weight, and blend composition) that are relevant to the production of the blend. Each of these factors can significantly impact the final properties of the SPE membrane, such as the conductivity, the electrochemical stability (in the following paragraph is indicated as voltage), as well as the crystallinity. The objective of our study is to systematically investigate the influence of these key factors on the production of a PEO/PC polymeric blend. About the type of PEO, we explored the effects induced by the variation of molecular weight using two distinct PEOs with M_w of $4 \cdot 10^5 \text{ g mol}^{-1}$ (400k) and $4 \cdot 10^6 \text{ g mol}^{-1}$ (4M) respectively, which can influence the blend's viscosity and chain entanglement. At the same time, we examined the influence of employing two different types of polycarbonates, *i.e.*, PEC and PPC. The blend composition ratio and the relative effects on the final properties were also investigated, varying the percentage of PEO (0, 30, 50, 70, and 100 %) in the formulation with PC. To evaluate the influence of these factors and their correlations, we used a Design of Experiment (DoE) approach, which offers several advantages over traditional one-factor-at-a-time experimentation [45]. A full factorial design was used to investigate the combination of experimental factors leading to the production of 20 different membranes ($2 \times 2 \times 5$ combinations) with four membranes prepared in replicate, to evaluate the experimental variability (full set of experiments is listed in Table S1). A multivariate analysis based on multiple linear regression (MLR) has been performed to quantify the effects of the experimental variables on the blend properties [46]. For each property (conductivity, voltage, and crystallinity), a regression model has been calculated (at a 90 % confidence level), in order to describe their variation over the investigated experimental domain.

3. Results and discussion

3.1. Thermal properties

Thermal analyses were performed to evaluate the thermal stability of the SPE membranes under study. TGA thermograms (Fig. S1) pointed out that PEO starts decomposing at around 370–375 °C for both M_w s, while PCs start decomposing at lower temperatures, namely 218 and 240 °C for PEC and PPC, respectively. The addition of LiTFSI influences the thermal stability of PEO and PCs differently. For PEO, the thermogram evidences a two-step decomposition at 380–390 and 430 °C, respectively. The first decomposition step, is related to the chain scission of the polymer. The second decomposition step is caused by the complexation of LiTFSI with ethylene oxide units [47,48]. On the contrary, a reduction to 200 °C of the decomposition onset was observed for

PCs. The reduction of the thermal stability of PCs is associated with the catalytic activity of LiTFSI in triggering the depolymerization process at high temperatures [49,50]. The overall effect of the PC addition is a slight reduction in the thermal stability of about 20 °C. However, all the compositions are thermally stable up to 190 °C, which is considered sufficient since the operative temperature of cells is not expected to exceed 100 °C, assuring high safety levels in normal conditions as well as in case of thermal runaways [51,52]. As expected, the thermograms of the PEO-PC mixtures evidence two main degradation steps, the first associated with PCs degradation and the second related to PEO and LiTFSI degradations. The mass loss relative to the two polymer degradations agrees with the ratio of PEO:PCs formulations introduced in the extruder. The residual mass at 600 °C is associated with the LiTFSI residue, and the differences among samples are related to the slightly different quantities of salt used to maintain the same [EO]:[Li] ratio at 20:1. DSC analyses were carried out to evaluate the effects of LiTFSI salt and the influence of PCs on the crystallinity degree (Fig. S2). Both types of neat PEO showed a crystallinity degree of 70 %, and the addition of LiTFSI salt halved the crystallinity, thanks to the high solubility and interaction of Li^+ with the polymeric chains and the plasticizing effect of TFSI⁻ anion [53]. The bis(fluorosulfonyl)imide anion interacts with PEO chains, preventing dense packing of the polymer segments and increasing the chain mobility [54,55]. This disruption of the crystalline structure increases the amorphous region within the polymer matrix. Moreover, the addition of amorphous polycarbonate effectively reduces the crystallinity as highlighted in Fig. 2; the melting peaks intensity decreases and shifts to lower temperatures when the polycarbonate ratio increases [56]. The multivariate analysis of the crystallinity values measured for the different blend compositions (Table 1) evidences that the amount of PEO is the sole relevant variable influencing this parameter (Fig. S4). In particular, the crystallinity degree decreases proportionally with the percentage of PEO in the blend. The predicted variation of crystallinity shows that the blend becomes completely amorphous at values equal to or lower than 40 % of PEO (Fig. 2). On the contrary, the molecular weight of PEO and the structural unit of PC did not seem to affect the resulting crystallinity. Among the two types of polycarbonates tested, the formulations containing PEC showed a higher reduction in crystallinity values, most likely associated with the lower T_g of the PEC polymer. Instead, slight variations, showing a general decrease in the T_α values (determined from DMA analysis), were observed across all formulations, as shown in Table 1. Generally, lower crystallinity and T_g are advantageous for using these polymeric membranes as electrolytes, as a reduced crystallinity is expected to increase the lithium-ion conductivity, particularly at room temperature. The presence of both relaxation peaks of PEO and PCs pointed out that the polymers are slightly soluble.

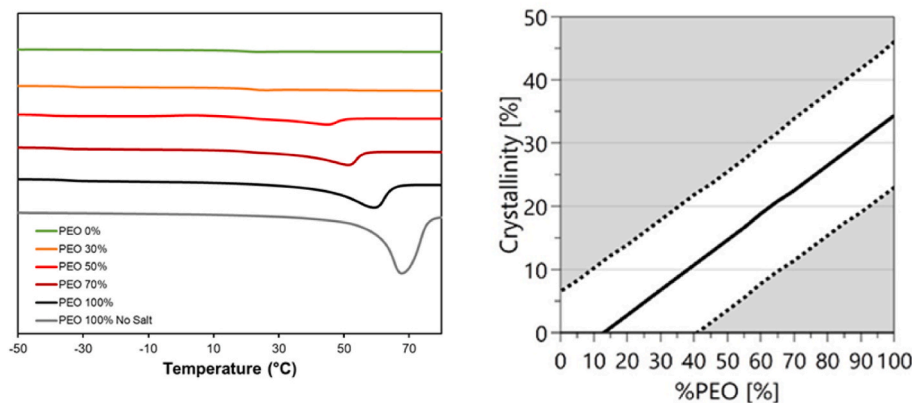


Fig. 2. DSC analysis of PEO/PEC blend under N_2 from -50 – 100 °C with a heating rate of 10 °C min^{-1} (left). Effect of the % of PEO on the crystallinity calculated from DoE analysis (right). In this case, the mathematical fitting goes below 0 % of crystallinity, which has no physical sense due to the impossibility of setting a lower limit.

Relevant information about the T_g values of the tested formulations can be obtained from DSC measurements, even if, in most cases, the melting peak overlaps the signal related to PC's T_g . Firstly, the addition of LiTFSI increased the T_g of PEO from -50 to -35 °C, as reported in the literature [57], whereas the T_g of PCs was less affected by the salt addition, changing from 14 to 20 °C for PEC and from 27 to 25 °C for PPC. The presence of two different T_g s is in agreement with the DMA analysis, confirming that PEO and PEC/PPC are not miscible, suggesting phase separation within the blend. Finally, these results demonstrate that the addition of PCs to the LiTFSI-PEO system allows to lower the crystallinity degree. It is well known that lower values of crystallinity promotes the migration of lithium ions, which in turn leads to higher ionic conductivity.

3.2. Thermo-mechanical and morphological characterization

DMA thermograms were performed in the temperature range from -60 to 60 °C for the formulation containing 50 wt% of PEC and PEO 400k, which can be compared to the pure PEO 400k formulation. Due to the quite similar storage and loss modulus values, resulting in limited significance in evaluating the best formulation, the DMA thermograms are considered only to assess the T_α of the materials (correspondingly, values are listed in Table 1). In this case, two different T_α can be pointed out for the two-component formulation, indicating a phase separation.

The films obtained after hot-pressing were flexible, self-standing, and homogeneous by naked-eye inspection. The morphologies of the three polymeric blends composed of PEO and PEC at varying weight ratios (30, 50, and 70 wt% of PEC) were investigated by SEM analysis. SEM images of the polymeric blends revealed that all three compositions exhibited a smooth and homogeneous surface. No distinct domains or phase boundaries attributable to PEO or PEC were observed at the reported magnification, irrespectively of the weight ratios (Fig. S3).

The micrographs obtained from the surface analysis displayed a uniform and continuous appearance, suggesting that the PEO and PEC components are well-homogenized at the microscale level. The cross-sectional study of the polymeric blends yielded results similar to the surface analysis. This indicates that the manufacturing process resulted in blends apparently homogenous at the microscale. However, the DSC and the DMA measurements indicate that the T_g of the polymers does not change after mixing, indicating that phase separation is present at a submicronic scale. The presence of the two phases is indeed expected for this type of blend, as reported by X-Y. Yu et al. [58]. The phase separation might be visible only at higher magnification, resolution and contrast compared to the SEM images obtained in the used experimental conditions. Unfortunately, attempts to obtain higher magnifications caused a significant visible degradation of the sample, precluding the

Table 1 T_{α} values (obtained from DMA) and percentage of crystallinity (obtained from DSC) for all samples.

PC (%)	PEO 4M/PEC formulations			PEO 4M/PPC formulations			PEO 400k/PEC formulations			PEO 400k/PPC formulations		
	T_{α} PEO (°C)	T_{α} PEC (°C)	Crystallinity (%)	T_{α} PEO (°C)	T_{α} PPC (°C)	Crystallinity (%)	T_{α} PEO (°C)	T_{α} PEC (°C)	Crystallinity (%)	T_{α} PEO (°C)	T_{α} PPC (°C)	Crystallinity (%)
0	-30	-	35	-30	-	35	-32	-	33	-32	-	33
30	-33	22	33	-34	37	19	-33	25	24	-34	36	22
50	-36	-	1	-31	40	9	-33	23	8	-31	39	11
70	-36	23	0	-33	40	0	-33	21	0	-32	40	0
100	-	21	0	-	26	0	-	21	0	-	26	0

investigation of submicronic phase separation. However, the detailed investigation of the phase separation at the nanoscale is out of the scope of the present work, which is related to investigating the thermal and electrochemical properties of the polymeric blends for solid-state Li-based battery application.

3.3. Ionic conductivity and electrochemical properties

The practical operation of SPEs is influenced by their ionic conductivity, which can be determined by electrochemical impedance spectroscopy (EIS) analysis. All Arrhenius plots of PEO/PC SPEs at different PEO contents in the temperature range of 0–80 °C are shown in Fig. S5, while Fig. 3 shows the conductivities of PEO 400k/PEC formulations.

At temperatures above 50 °C, PEO displayed similar conductivity to the blends due to the melting of crystalline domains occurring at around 50 °C. Above this temperature, the material is completely amorphous, which improves ion mobility. However, at lower temperatures, the electrolytes made of PEO/PC show better ionic conductivity compared to the pure PEO. This is related to the reduction in crystallinity of PEO in the system, as demonstrated by the DSC thermograms. Thus, the blend of PEO with amorphous PCs at lower temperatures possesses higher ion conduction properties.

Moreover, the curve slope in the high-temperature region (80–50 °C) is different from that in the low-temperature region (50–0 °C). The reason behind this effect is the recrystallization of PEO that occurs at temperatures lower than 50 °C. This behaviour is less pronounced in the curves of the PEO/PC blends due to the lower crystallinity of these systems. The σ_i values at 40 °C are shown in Fig. 3B. In addition, it is observable that in all blends, SPEs with PEO 400k showed slightly higher conductivity compared to those containing PEO 4M. Low molecular weight PEO has shorter polymer chains, which generally result in higher segmental mobility [59]. This increased mobility facilitates ion transport, enhancing ionic conductivity. This behaviour agrees with the study of Teran et al., who found that the conductivity is proportional to $1/M_w$ in a PEO/LiTFSI electrolyte [60].

The effects of PC and PEO types, as well as the weight percentage of PEO, on the conductivity were evaluated at 40 °C through DoE analysis.

Among them, the main influential variable is the percentage of PEO in the blend (Fig. S4). Generally, conductivity values at 40 °C improved from 10^{-9} to 10^{-5} S cm⁻¹ with increasing the quantity of PEO from 0 to 50 %, respectively. The blends with 50 % of PCs provided the best conductivity in the range of 10^{-5} S cm⁻¹ at 40 °C. This value is comparable with the PEO and PCs electrolyte obtained by co-polymerization or solvent casting blend reported by others [61,62]. Above such percentage, the values remained relatively stable, and only a slight decrease is observed with pure PEO (Fig. 3C). In addition to % PEO, the type of PC shows a minor effect on the conductivity, where the use of PEC, instead of PPC, leads to slightly higher values. Contrarily to previous observations, molecular weight is not considered a significant factor in DoE analysis. Among all the polyelectrolytes tested, PEO 400k:PEC 1:1 exhibited the highest ionic conductivity (4.584×10^{-5} S cm⁻¹).

When comparing SPEs with the same PC content, it is evident that the type of PC plays a role in determining ionic conductivity. PEC-based membranes generally exhibited higher conductivity compared to PPC-based ones, which is likely attributed to the intrinsic higher conductivity of the pure PEC, which is higher than PPC (Fig. S5). Moreover, the molecular weight of PEO influenced the conductivity of the electrolyte when considering samples with only PEO. Despite a high conductivity of PEO 4M, SPEs with PEO 400k showed close conductivity compared to the same blends made with PEO 4M.

The electrochemical stability window (ESW) of PEO/PC blends was evaluated using linear sweep voltammetry (LSV) at 40 °C. By applying this characterization technique, we aimed to demonstrate the potential for electrolyte degradation up to a certain cut-off voltage. We compared the oxidation stability of all blends to observe any effects resulting from the factors we examined. The results of the LSV curve for the blend of PEO 4M and PEC are shown in Fig. 4A. It can be observed that the potential of neat PEO-based SPE starts to increase around 4.3 V (vs. Li⁺/Li), and as the voltage is increased, the oxidation current increases sharply. However, it is evident that upon the addition of amorphous PEC, the voltage at which oxidative decomposition takes place increases gradually. A value of 4.64 V (vs. Li⁺/Li) is reached when 70 % of PEC is added. These findings indicate that the electrochemical stability of blend SPEs can be enhanced by adding PEC, with the stability improvement being

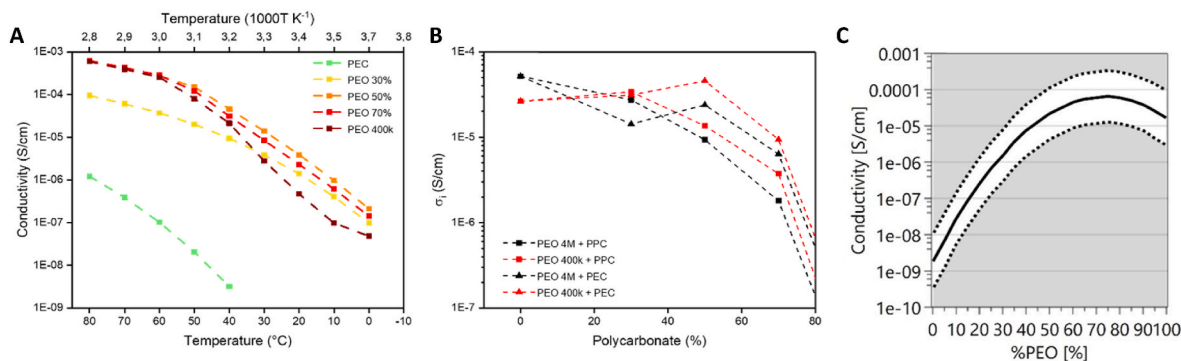


Fig. 3. Arrhenius plots of ionic conductivity versus inverse temperature determined by EIS in the range of 0–80 °C for PEO 400k/PEC formulations (A). Comparison of the conductivity values at 40 °C varying the percentage of polycarbonate in the blend (B). Effect of the % PEO on the conductivity calculated from DoE analysis (C).

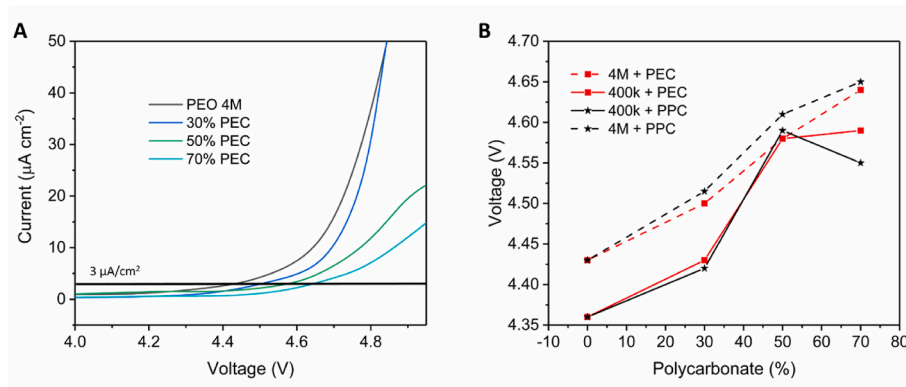


Fig. 4. Linear sweep voltammetry (LSV) for neat PEO and PEO-PEC blends (A). Comparison of the voltage value varying the percentage of polycarbonate; cut-off: $3 \mu\text{A cm}^{-2}$ (B).

directly related to PEC content. This enhancement is attributed to the wide ESW of PCs [31]. Notably, the oxidation peak of water is not observable in all samples, meaning that the drying process is efficient enough to remove all traces of water that can eventually be contained in both PEO and LiTFSI components.

Then, the oxidation stability was evaluated for all the blends; Fig. 4B shows the voltage stability evaluated at the threshold of a leak current of $3 \mu\text{A cm}^{-2}$. The evaluation has excluded the LSV of pure PC membranes due to the much lower ionic conductivity at 40°C of polycarbonates, which influences the obtained values. For this reason, it was not possible to conduct a multivariate analysis for this parameter because of the lack of data. The figure shows that the % PC is the most influential variable. Among the experimental trials, PEO 4M:PPC 3:7 exhibited the highest electrochemical stability (4.65 V). Varying the weight ratio of PEO and PC within the polymeric blend leads to a variation in the electrochemical stability with a general improvement, reaching a maximum around the ratio 3:7 of PEO/PC. On the contrary, PC type and PEO's molecular weight have a lower impact on the voltage stability. Varying the molecular weight of PEO was shown to influence the voltage stability, with blends containing PEO 4M displaying better stability. Differently, the type of PC has a lower influence on the oxidation potential, and the SPEs containing PPC are proven to have slightly better electrochemical stability. This result, along with no substantial weight loss at around 100°C in the TGA, suggests that the extrusion process allowed the production of salt-in-polymer blends without water contamination or degradation of the polymers, with promising prospects as SPEs in Li-based batteries.

4. Conclusions

In this work, a series of SPEs was developed by incorporating two types of polycarbonates, *viz.* polyethylene and polypropylene carbonate, in a PEO-based matrix encompassing LiTFSI salt. Different molecular weight PEOs and compositions (from 0 to 100 % of PEO) were investigated to optimize the final polyelectrolyte properties, such as crystallinity, electrochemical stability window, and ionic conductivity. Blend SPEs were successfully produced by employing a mini-compounder to mix the precursors materials in one pot, homogeneously and efficiently. The process developed can be easily scaled up, finding industrial applications and avoiding the use of organic solvents. Homogeneous mixing of the component was confirmed by SEM images, which did not reveal any distinct domain at the micrometer scale. We observed that the addition of amorphous PC led to a substantial decrease in crystallinity, which is attested to around 10 % when 50 % of PEO is used. No relevant effect was induced by the type of PC used. Also, all blends exhibited improved ionic conductivity up to a threshold of 50 % of PEO, while further decrease in the PEO percentage was detrimental to conductivity. The sample PEO400k, with 50 % of PEC, displayed the best ionic conductivity among the series with $4.6 \times 10^{-5} \text{ S cm}^{-1}$ at 40°C , showing an

increase of 57 % with respect to the SPE with only PEO 400k. The ESW also took advantage of the addition of PCs, reaching a maximum in the anodic stability for the formulation with 70 % of PEO. Enhanced breakdown value of 4.65 V was reached for PEO 4M with 70 % of PPC, indicating a beneficial role of PCs. The statistical analyses of the experimental results within a DoE approach confirmed that the most important parameter that should be taken into account is the quantity of PEO, showing an excellent trade-off among all properties for a ratio of PEO 400k:PEC 1:1. The possibility of readily scale up the solvent-free production process and the improved mechanical and electrochemical performances make the LiTFSI-PEO/PC blended SPE a promising candidate for next-generation solid-state Li-based energy storage technologies.

CRediT authorship contribution statement

Francesco Gambino: Writing – review & editing, Writing – original draft, Investigation, Formal analysis, Data curation. **Matteo Gastaldi:** Writing – review & editing, Writing – original draft, Formal analysis, Data curation, Conceptualization. **Alia Jouhara:** Writing – review & editing. **Samuel Malburet:** Writing – review & editing. **Simone Galliano:** Writing – review & editing, Formal analysis, Data curation. **Nicola Cavallini:** Writing – review & editing, Formal analysis, Data curation. **Giovanna Colucci:** Writing – review & editing, Formal analysis, Data curation. **Marco Zanetti:** Writing – review & editing, Formal analysis, Data curation. **Alberto Fina:** Writing – review & editing, Formal analysis, Data curation. **Giuseppe Antonio Elia:** Writing – review & editing, Writing – original draft, Supervision, Methodology, Funding acquisition, Conceptualization. **Claudio Gerbaldi:** Writing – review & editing, Writing – original draft, Supervision, Project administration, Funding acquisition, Formal analysis, Data curation, Conceptualization.

Declaration of competing interest

The authors declare no conflict of interest statement.

Acknowledgements

The PSIONIC project has received funding from the European Union's Horizon Europe Research and Innovation Programme under Grant Agreement N. 101069703. This study was carried out under the National Recovery and Resilience Plan (NRRP), within the MOST – Sustainable Mobility Center and received funding from the European Union Next-GenerationEU (PIANO NAZIONALE DI RIPRESA E RESILIENZA – PNRR eMission 4, Component 2, Investment 1.4 and D.D. 1033 17/06/2022 of the Ministero dell'Università e della Ricerca (MUR), CN00000023, POC HYLESS). This manuscript reflects only the authors'

views and opinions, neither the European Union nor the European Commission can be considered responsible for them. The authors acknowledge the program Piano Triennale della Ricerca (PTR) within "Ricerca Sistema Elettrico Nazionale 2022–2024" funded through contributions to research and development by the Italian Ministry of Economic Development.

Appendix A. Supplementary data

Supplementary data to this article can be found online at <https://doi.org/10.1016/j.powera.2024.100160>.

Data availability

No data was used for the research described in the article.

References

- J.B. Goodenough, K.S. Park, The Li-ion rechargeable battery: a perspective, *J. Am. Chem. Soc.* 135 (2013) 1167–1176, <https://doi.org/10.1021/ja3091438>.
- B. Dunn, H. Kamath, J.-M. Tarascon, Electrical energy storage for the grid: a battery of choices, *Science* 334 (2011) 928–935, <https://doi.org/10.1126/science.1212741>.
- T. Cai, Y. Wang, F. Zhao, Z. Ma, P. Kumar, H. Xie, C. Sun, J. Wang, Q. Li, Y. Guo, J. Ming, Graphic, quantitation, visualization, standardization, digitization, and intelligence of electrolyte and electrolyte-electrode interface, *Adv. Energy Mater.* 14 (2024), <https://doi.org/10.1002/aenm.202400569>.
- S. Zhang, K. Ueno, K. Dokko, M. Watanabe, Recent advances in electrolytes for lithium-sulfur batteries, *Adv. Energy Mater.* 5 (2015), <https://doi.org/10.1002/aenm.201500117>.
- J.I. Lee, M. Shin, D. Hong, S. Park, Efficient Li-Ion-Conductive layer for the realization of highly stable high-voltage and high-capacity lithium metal batteries, *Adv. Energy Mater.* 9 (2019), <https://doi.org/10.1002/aenm.201803722>.
- Y. Liu, D. Lin, Z. Liang, J. Zhao, K. Yan, Y. Cui, Lithium-coated polymeric matrix as a minimum volume-change and dendrite-free lithium metal anode, *Nat. Commun.* 7 (2016), <https://doi.org/10.1038/ncomms10992>.
- Y. Chen, Z. Ma, Y. Wang, P. Kumar, F. Zhao, T. Cai, Z. Cao, L. Cavallo, H. Cheng, Q. Li, J. Ming, Trace ethylene carbonate-mediated low-concentration ether-based electrolytes for high-voltage lithium metal batteries, *Energy Environ. Sci.* (2024), <https://doi.org/10.1039/d4ee01831a>.
- H. Liang, Z. Ma, Y. Wang, F. Zhao, Z. Cao, L. Cavallo, Q. Li, J. Ming, Solvent-solvent interaction mediated lithium-ion (De)intercalation chemistry in propylene carbonate based electrolytes for lithium-sulfur batteries, *ACS Nano* 17 (2023) 18062–18073, <https://doi.org/10.1021/acsnano.3c04790>.
- D. Lv, Y. Shao, T. Lozano, W.D. Bennett, G.L. Graff, B. Polzin, J. Zhang, M. H. Engelhard, N.T. Saenz, W.A. Henderson, P. Bhattacharya, J. Liu, J. Xiao, Failure mechanism for fast-charged lithium metal batteries with liquid electrolytes, *Adv. Energy Mater.* 5 (2015), <https://doi.org/10.1002/aenm.201400993>.
- X. Zheng, L. Huang, X. Ye, J. Zhang, F. Min, W. Luo, Y. Huang, Critical effects of electrolyte recipes for Li and Na metal batteries, *Chem* 7 (2021) 2312–2346, <https://doi.org/10.1016/j.chempr.2021.02.025>.
- A. Manthiram, X. Yu, S. Wang, Lithium battery chemistries enabled by solid-state electrolytes, *Nat. Rev. Mater.* 2 (2017), <https://doi.org/10.1038/natrevmats.2016.103>.
- Q. Zhao, S. Stalin, C.Z. Zhao, L.A. Archer, Designing solid-state electrolytes for safe, energy-dense batteries, *Nat. Rev. Mater.* 5 (2020) 229–252, <https://doi.org/10.1038/s41578-019-0165-5>.
- L. Fan, S. Wei, S. Li, Q. Li, Y. Lu, Recent progress of the solid-state electrolytes for high-energy metal-based batteries, *Adv. Energy Mater.* 8 (2018), <https://doi.org/10.1002/aenm.201702657>.
- Y. An, X. Han, Y. Liu, A. Azhar, J. Na, A.K. Nanjundan, S. Wang, J. Yu, Y. Yamauchi, Progress in solid polymer electrolytes for lithium-ion batteries and beyond, *Small* 18 (2022), <https://doi.org/10.1002/smll.202103617>.
- L. Long, S. Wang, M. Xiao, Y. Meng, Polymer electrolytes for lithium polymer batteries, *J Mater Chem A Mater* 4 (2016) 10038–10039, <https://doi.org/10.1039/c6ta02621d>.
- D.E. Fenton, J.M. Parker, P.V. Wright, Complexes of alkali metal ions with poly(ethylene oxide), *Polymer (Guilf)* 14 (1973).
- M. Armand, Polymer solid electrolytes - an overview, *Solid State Ion* 9–10 (1983) 745–754, [https://doi.org/10.1016/0167-2738\(83\)90083-8](https://doi.org/10.1016/0167-2738(83)90083-8).
- W. Zhou, Z. Wang, Y. Pu, Y. Li, S. Xin, X. Li, J. Chen, J.B. Goodenough, Double-layer polymer electrolyte for high-voltage all-solid-state rechargeable batteries, *Adv. Mater.* 31 (2019), <https://doi.org/10.1002/adma.201805574>.
- G. Wang, X. Zhu, A. Rashid, Z. Hu, P. Sun, Q. Zhang, L. Zhang, Organic polymeric filler-amorphized poly(ethylene oxide) electrolyte enables all-solid-state lithium-metal batteries operating at 35 °C, *J Mater Chem A Mater* 8 (2020) 13351–13363, <https://doi.org/10.1039/d0ta00335b>.
- J. Mindemark, M.J. Lacey, T. Bowden, D. Brandell, Beyond PEO—alternative host materials for Li⁺-conducting solid polymer electrolytes, *Prog. Polym. Sci.* 81 (2018) 114–143, <https://doi.org/10.1016/j.progpolymsci.2017.12.004>.
- Z. Xue, D. He, X. Xie, Poly(ethylene oxide)-based electrolytes for lithium-ion batteries, *J Mater Chem A Mater* 3 (2015) 19218–19253, <https://doi.org/10.1039/c5ta03471j>.
- L. Stolz, S. Hochstädt, S. Röser, M.R. Hansen, M. Winter, J. Kasnatscheew, Single-ion versus dual-ion conducting electrolytes: the relevance of concentration polarization in solid-state batteries, *ACS Appl. Mater. Interfaces* 14 (2022) 11559–11566, <https://doi.org/10.1021/acsmi.2c00084>.
- H.M.J.C. Pitawala, M.A.K.L. Dissanayake, V.A. Seneviratne, B.E. Mellander, I. Albinson, Effect of plasticizers (EC or PC) on the ionic conductivity and thermal properties of the (PEO)₉LiTf: Al₂O₃ nanocomposite polymer electrolyte system, in: *Journal of Solid State Electrochemistry*, Springer Science and Business Media, LLC, 2008, pp. 783–789, <https://doi.org/10.1007/s10008-008-0505-7>.
- W. Liu, S.W. Lee, D. Lin, F. Shi, S. Wang, A.D. Sendek, Y. Cui, Enhancing ionic conductivity in composite polymer electrolytes with well-aligned ceramic nanowires, *Nat. Energy* 2 (2017), <https://doi.org/10.1038/nenergy.2017.35>.
- C. Tao, M.H. Gao, B.H. Yin, B. Li, Y.P. Huang, G. Xu, J.J. Bao, A promising TPU/PEO blend polymer electrolyte for all-solid-state lithium ion batteries, *Electrochim. Acta* 257 (2017) 31–39, <https://doi.org/10.1016/j.electacta.2017.10.037>.
- B. Zhang, Y. Liu, X. Pan, J. Liu, K. Doyle-Davis, L. Sun, J. Liu, X. Jiao, J. Jie, H. Xie, X. Sun, Dendrite-free lithium metal solid battery with a novel polyester based triblock copolymer solid-state electrolyte, *Nano Energy* 72 (2020), <https://doi.org/10.1016/j.nanoen.2020.104690>.
- L. Porcarelli, C. Gerbaldi, F. Bella, J.R. Nair, Super soft all-ethylene oxide polymer electrolyte for safe all-solid lithium batteries, *Sci. Rep.* 6 (2016), <https://doi.org/10.1038/srep19892>.
- G. Lingua, P. Grysan, P.S. Vlasov, P. Verge, A.S. Shaplov, C. Gerbaldi, Unique carbonate-based single ion conducting block copolymers enabling high-voltage, all-solid-state lithium metal batteries, *Macromolecules* 54 (2021) 6911–6924, <https://doi.org/10.1021/acs.macromol.1c00981>.
- H. Zhang, C. Li, M. Piszcz, E. Coya, T. Rojo, L.M. Rodriguez-Martinez, M. Armand, Z. Zhou, Single lithium-ion conducting solid polymer electrolytes: advances and perspectives, *Chem. Soc. Rev.* 46 (2017) 797–815, <https://doi.org/10.1039/c6cs00491a>.
- B. Sun, J. Mindemark, K. Edström, D. Brandell, Polycarbonate-based solid polymer electrolytes for Li-ion batteries, *Solid State Ion* 262 (2014) 738–742, <https://doi.org/10.1016/j.ssi.2013.08.014>.
- Z. Li, J. Mindemark, D. Brandell, Y. Tominaga, A concentrated poly(ethylene carbonate)/poly(trimethylene carbonate) blend electrolyte for all-solid-state Li battery, *Polym. J.* 51 (2019) 753–760, <https://doi.org/10.1038/s41428-019-0184-5>.
- J. Mindemark, B. Sun, D. Brandell, Hydroxyl-functionalized poly(trimethylene carbonate) electrolytes for 3D-electrode configurations, *Polym. Chem.* 6 (2015) 4766–4774, <https://doi.org/10.1039/c5py00446b>.
- K. Kimura, J. Motomatsu, Y. Tominaga, Highly concentrated polycarbonate-based solid polymer electrolytes having extraordinary electrochemical stability, *J. Polym. Sci. B Polym. Phys.* 54 (2016) 2442–2447, <https://doi.org/10.1002/polb.24235>.
- P.N. Didwal, Y.N. Singhhbabu, R. Verma, B.J. Sung, G.H. Lee, J.S. Lee, D.R. Chang, C.J. Park, An advanced solid polymer electrolyte composed of poly(propylene carbonate) and mesoporous silica nanoparticles for use in all-solid-state lithium-ion batteries, *Energy Storage Mater.* 37 (2021) 476–490, <https://doi.org/10.1016/j.jensm.2021.02.034>.
- K. Xu, Nonaqueous liquid electrolytes for lithium-based rechargeable batteries, *Chem Rev* 104 (2004) 4303–4417, <https://doi.org/10.1021/cr032020g>.
- B. Sun, J. Mindemark, K. Edström, D. Brandell, Polycarbonate-based solid polymer electrolytes for Li-ion batteries, *Solid State Ion* 262 (2014) 738–742, <https://doi.org/10.1016/j.ssi.2013.08.014>.
- L. Zhu, J. Li, Y. Jia, P. Zhu, M. Jing, S. Yao, X. Shen, S. Li, F. Tu, Toward high performance solid-state lithium-ion battery with a promising PEO/PPC blend solid polymer electrolyte, *Int. J. Energy Res.* 44 (2020) 10168–10178, <https://doi.org/10.1002/er.5632>.
- Y.C. Jung, M.S. Park, D.H. Kim, M. Ue, A. Eftekhari, D.W. Kim, Room-temperature performance of poly(ethylene ether carbonate)-based solid polymer electrolytes for all-solid-state lithium batteries, *Sci. Rep.* 7 (2017), <https://doi.org/10.1038/s41598-017-17697-0>.
- B. Ludwig, Z. Zheng, W. Shou, Y. Wang, H. Pan, Solvent-free manufacturing of electrodes for lithium-ion batteries, *Sci. Rep.* 6 (2016), <https://doi.org/10.1038/srep23150>.
- A. Mejía, S. Devaraj, J. Guzmán, J.M. Lopez Del Amo, N. García, T. Rojo, M. Armand, P. Tiemblo, Scalable plasticized polymer electrolytes reinforced with surface-modified sepiolite fillers - a feasibility study in lithium metal polymer batteries, *J. Power Sources* 306 (2016) 772–778, <https://doi.org/10.1016/j.jpowsour.2015.12.099>.
- L. Helmers, L. Froböse, K. Friedrich, M. Steffens, D. Kern, P. Michalowski, A. Kwade, Sustainable solvent-free production and resulting performance of polymer electrolyte-based all-solid-state battery electrodes, *Energy Technol.* 9 (2021), <https://doi.org/10.1002/ente.202000923>.
- Z. Li, A.M. Aboalsaud, X. Liu, R.L. Thankamony, I.C. Chen, Y. Li, Z. Lai, Scalable fabrication of solvent-free composite solid electrolyte by a continuous Thermal-Extrusion process, *J. Colloid Interface Sci.* 628 (2022) 64–71, <https://doi.org/10.1016/j.jcis.2022.07.099>.
- E. Martuscelli, C. Silvestre, M.L. Addonizio, L. Amelino, Phase structure and compatibility studies in poly(ethylene oxide)/poly(methyl methacrylate) blends, *Makromol. Chem.* 187 (1986) 1557–1571.
- X. Wen, Y. Su, S. Li, W. Ju, D. Wang, Isothermal crystallization kinetics of poly(ethylene oxide)/poly(ethylene glycol)-g-silica nanocomposites, *Polymers* 13 (2021) 1–16, <https://doi.org/10.3390/polym13040648>.

- [45] R. Leardi, Experimental design in chemistry: a tutorial, *Anal. Chim. Acta* 652 (2009) 161–172, <https://doi.org/10.1016/j.aca.2009.06.015>.
- [46] M. Sergent, D. Mathieu, R. Phan-Tan-Luu, G. Drava, Chemometrics and Intelligent Laboratory Systems Tutorial Correct and Incorrect Use of Multilinear Regression, 1995.
- [47] Y. Tominaga, V. Nanthana, D. Tohyama, Ionic conduction in poly(ethylene carbonate)-based rubbery electrolytes including lithium salts, *Polym. J.* 44 (2012) 1155–1158, <https://doi.org/10.1038/pj.2012.97>.
- [48] B.N. Choi, J.H. Yang, Y.S. Kim, C.H. Chung, Effect of morphological change of copper-oxide fillers on the performance of solid polymer electrolytes for lithium-metal polymer batteries, *RSC Adv.* 9 (2019) 21760–21770, <https://doi.org/10.1039/c9ra03555a>.
- [49] B. Commarieu, A. Paoletta, S. Collin-Martin, C. Gagnon, A. Vijn, A. Guerfi, K. Zaghib, Solid-to-liquid transition of polycarbonate solid electrolytes in Li-metal batteries, *J. Power Sources* 436 (2019), <https://doi.org/10.1016/j.jpowsour.2019.226852>.
- [50] A. Buchheit, M. Grünebaum, B. Teßmer, M. Winter, H.D. Wiemhöfer, Polycarbonate-based lithium salt-containing electrolytes: new insights into thermal stability, *J. Phys. Chem. C* 125 (2021) 4371–4378, <https://doi.org/10.1021/acs.jpcc.0c09968>.
- [51] K. Kimura, J. Hassoun, S. Panero, B. Scrosati, Y. Tominaga, Electrochemical properties of a poly(ethylene carbonate)-LiTFSI electrolyte containing a pyrrolidinium-based ionic liquid, *Ionics* 21 (2015) 895–900, <https://doi.org/10.1007/s11581-015-1370-x>.
- [52] L. Porcarelli, C. Gerbaldi, F. Bella, J.R. Nair, Super soft all-ethylene oxide polymer electrolyte for safe all-solid lithium batteries, *Sci. Rep.* 6 (2016), <https://doi.org/10.1038/srep19892>.
- [53] H. Zhang, C. Liu, L. Zheng, F. Xu, W. Feng, H. Li, X. Huang, M. Armand, J. Nie, Z. Zhou, Lithium bis(fluorosulfonyl)imide/poly(ethylene oxide) polymer electrolyte, *Electrochim. Acta* 133 (2014) 529–538, <https://doi.org/10.1016/j.electacta.2014.04.099>.
- [54] H. Zhang, C. Liu, L. Zheng, F. Xu, W. Feng, H. Li, X. Huang, M. Armand, J. Nie, Z. Zhou, Lithium bis(fluorosulfonyl)imide/poly(ethylene oxide) polymer electrolyte, *Electrochim. Acta* 133 (2014) 529–538, <https://doi.org/10.1016/j.electacta.2014.04.099>.
- [55] A. Vallée, S. Besner, J. Prud'homme, COMPARATIVE STUDY OF POLY(ETHYLENE OXIDE) ELECTROLYTES MADE WITH LiN(CF₃SO₂), LiCF₃SO₃, AND LiClO₄: thermal properties and conductivity behaviour, *Electrochimica Acta* 37 (1992) 1579–1583.
- [56] C. Li, Q. Kong, Q. Fan, Y. Xia, Crystallization behavior of polycarbonate/poly(ethylene oxide) blends studied by DSC, *Mater. Lett.* 59 (2005) 773–778, <https://doi.org/10.1016/j.matlet.2004.11.018>.
- [57] M. Polaskova, P. Peer, R. Cermak, P. Ponizil, Effect of thermal treatment on crystallinity of poly(ethylene oxide) electrospun fibers, *Polymers* 11 (2019), <https://doi.org/10.3390/polym11091384>.
- [58] Y. Xiao-Yuan, M. Xiao, W. Shuang-Jin, Z. Qi-Qiang, M. Yue-Zhong, Fabrication and characterization of peo/ppc polymer electrolyte for lithium-ion battery, *J. Appl. Polym. Sci.* 115 (2010) 2718–2722, <https://doi.org/10.1002/app.29915>.
- [59] K. Hayamizu, E. Akiba, T. Bando, Y. Aihara, ¹H, ⁷Li, and ¹⁹F nuclear magnetic resonance and ionic conductivity studies for liquid electrolytes composed of glymes and polyethenylene glycol dimethyl ethers of CH₃O(CH₂CH₂O)_nCH₃ (n = 3 - 50) doped with LiN(SO₂CF₃)₂, *J. Chem. Phys.* 117 (2002) 5929–5939, <https://doi.org/10.1063/1.1501279>.
- [60] A.A. Teran, M.H. Tang, S.A. Mullin, N.P. Balsara, Effect of molecular weight on conductivity of polymer electrolytes, *Solid State Ion* 203 (2011) 18–21, <https://doi.org/10.1016/j.ssi.2011.09.021>.
- [61] L. Meabe, T.V. Huynh, N. Lago, H. Sardon, C. Li, L.A. O'Dell, M. Armand, M. Forsyth, D. Mecerreyes, Poly(ethylene oxide carbonates) solid polymer electrolytes for lithium batteries, *Electrochim. Acta* 264 (2018) 367–375, <https://doi.org/10.1016/j.electacta.2018.01.101>.
- [62] W. He, Z. Cui, X. Liu, Y. Cui, J. Chai, X. Zhou, Z. Liu, G. Cui, Carbonate-linked poly(ethylene oxide) polymer electrolytes towards high performance solid state lithium batteries, *Electrochim. Acta* 225 (2017) 151–159, <https://doi.org/10.1016/j.electacta.2016.12.113>.